Bioconjugate Chemistry

Article

Cite This: Bioconjugate Chem. 2018, 29, 905−913

pubs.acs.org/bc

Reversible Control of Network Properties in Azobenzene-Containing Hyaluronic Acid-Based Hydrogels

Adrianne M. Rosales,*[,†,§] Christopher B. Rodell,[‡,∥] Minna H. Chen,[‡] Matthew G. Morrow,[‡] Kristi S. Anseth,[†] and Jason A. Burdick[‡]

[†]Department of Chemical and Biological Engineering & BioFrontiers Institute, University of Colorado Boulder, Boulder, Colorado 80303, United States

[‡]Department of Bioengineering, University of Pennsylvania, Philadelphia, Pennsylvania 19104, United States

Supporting Information

ABSTRACT: Biomimetic hydrogels fabricated from biologically derived polymers, such as hyaluronic acid (HA), are useful for numerous biomedical applications. Due to the dynamic nature of biological processes, it is of great interest to synthesize hydrogels with dynamically tunable network properties where various functions (e.g., cargo delivery, mechanical signaling) can be changed over time. Among the various stimuli developed to control hydrogel properties, light stands out for its exquisite spatiotemporal control; however, most light-based chemistries are unidirectional in their ability to manipulate network changes. Here, we report a strategy to reversibly modulate HA hydrogel properties with light, using supramolecular cross-links formed via azobenzene bound to *β*-cyclodextrin. Upon isomerization with 365 nm or 400−500 nm light, the binding affinity between azobenzene and *β*-cyclodextrin changed and altered the network connectivity. The hydrogel mechanical properties depended on both the azobenzene modification and isomeric state (lower for *cis* state), with up to a 60% change in storage modulus with light exposure. Furthermore, the release of a fluorescently labeled protein was accelerated with light exposure under conditions that were cytocompatible to encapsulated cells. These results indicate that the developed hydrogels may be suitable for applications in which temporal regulation of material properties is important, such as drug delivery or mechanobiology studies.

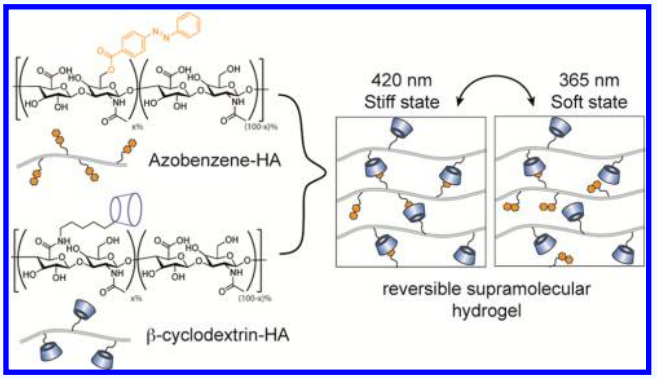

INTRODUCTION

Many biological phenomena are dynamic, such as disease progression or wound healing.[1] Advanced biomaterial approaches to mimic or treat these processes often necessitate systems in which the properties of interest can be controlled over time − for example, drug delivery systems in which the dose can be tuned "on demand" with an intrinsic or external trigger. Recent developments in hydrogel and biomaterial design have led to a number of strategies where network properties can be altered in a dynamic and also *reversible* manner.[2] For example, hydrogel cross-link density can be either increased or decreased (or both) in response to user-directed cues such as light,[3−6] temperature,[7] pH,[8] or external fields,[9] all of which can modulate molecular association within the hydrogel cross-links. Other strategies rely on mechanisms that confer a change in polymer conformation or persistence length, leading to changes in the distance between cross-links (and therefore cross-linking density); these include ligand binding to control polymer coordination,[10,11] DNA hybridization,[12] and protein folding/unfolding.[13−17] Here, we took a complementary approach to synthesize hydrogels with dynamic and reversibly tunable properties by controlling the *number* of elastically active cross-links via disrupting and reforming supramolecular interactions with light.

Light offers many desirable qualities as a stimulus to manipulate hydrogel properties, especially its high degree of spatiotemporal control and facile tunability of the dose introduced to biological systems. To generate photoresponsive cross-links, we utilized a photoisomer, azobenzene. Because azobenzene absorbs light in a wavelength range that is compatible with live cells (350−550 nm) to convert between its *trans* and *cis* isomers,[18] this photoisomerization can be leveraged to alter material properties with cells present. Previous efforts with azobenzene-modified hydrogels have resulted in materials with changes in mechanics[19] or cross-link density,[20] but modest change for many biological processes, although some have shown potential for biological applications.[21,22] Here, rather than solely changing molecular conformation in covalently cross-linked hydrogels, our

Special Issue: Biomimetic Materials

Received: December 15, 2017
Revised: February 2, 2018
Published: February 6, 2018

DOI: 10.1021/acs.bioconjchem.7b00802
Bioconjugate Chem. 2018, 29, 905−913

approach was to use azobenzene to control the association of noncovalent, reversible cross-links. In contrast to prior reports,[23] we also sought to maximize the change in number of cross-links without causing a gel−sol transition. This property could potentially enable applications of these materials as 3D cell culture matrices.

Azobenzene has an affinity for the hydrophobic cavity of cyclodextrin, allowing for the formation of a noncovalent guest−host linkage that can be disrupted upon conversion to the *cis* isomer when azobenzene is irradiated with ultraviolet light.[24,25] This type of linkage has been used to form supramolecular hydrogels that can convert from the gel phase to the sol phase with light,[26,27] and it has also been used to control ligand presentation to mediate biological interactions (e.g., cell adhesion).[28−30] Here, we sought to implement this interaction into reversible hydrogels that do not undergo a gel−sol transition and to develop a fundamental understanding of the structure−property relationship in azobenzene-cyclodextrin hyaluronic acid (HA) hydrogels.

In this work, we present the development of a hydrogel with azobenzene-containing guest−host cross-links to reversibly control network properties with light. The precursors are readily synthesized from HA and self-assemble into supramolecular hydrogels upon mixing at physiological conditions, even in the presence of cells. We demonstrate that the binding affinity of the guest−host cross-links can be modulated with mild exposure to defined wavelengths of light, leading to significant changes in cross-link density that result in up to a 2-fold change in the shear modulus. This strategy leads to a dynamic hydrogel in which the changes in network properties are decoupled from changes in chemical composition, thereby conferring the potential for well-defined studies in cellular mechanosensing or tissue engineering. In addition, we demonstrate the potential to leverage reversible changes in cross-link density for release of encapsulated proteins. The irradiation doses used here have previously been shown to be compatible with *in vivo* applications,[31] though the shorter wavelength (365 nm) may limit subcutaneous implantation of these materials (alternatives could include a skin adhesive patch). Altogether, these results indicate a feasible route to the dynamic control of hydrogels in the context of a biomimetic approach to material design.

RESULTS AND DISCUSSION

Hydrogel Design through Guest−Host Interactions. Four photoresponsive guest−host pairs were investigated as potential cross-linkers for the synthesis of supramolecular hydrogels. The binding affinity (K_a) between the guest and host determines the strength of the cross-links in supramolecular hydrogels, so we sought to identify a pair with a high enough K_a to lead to gelation, but that would also provide reversibility to formed hydrogels. Thus, HA polymers of 75 kDa were functionalized with either one of two different azobenzenes (Azo, 4-phenylazobenzoic acid or 3,3′-Azo, 3,3′-phenylazodibenzoic acid) or one of two different cyclodextrins (CD, α-CD or β-CD). The choice of guest Azo molecules allowed us to investigate the effect of of hydrogen bonding on affinity with the CD host. Binding affinities of the various pairs were measured using absorbance spectroscopy (Figure S3). Of the two Azo groups, HA functionalized with the more hydrophobic 4-phenylazobenzoic acid was found to have an overall higher K_a than HA functionalized with 3,3′-phenylazodibenzoic acid, regardless of the host molecule. The two hosts investigated, α-CD and β-CD, have varied inner diameters of 5.7 and 7.8 Å, respectively. The α-CD guest−host pairs exhibited higher binding affinities, likely due to the better size association between the guest and host. These results are summarized in Table 1.

Table 1. Binding Affinity of HA Polymers Modified with Various Guest−Host Pairs

	α-CD	β-CD
$Azo_{20}HA$	1900 ± 150 M^{-1}	760 ± 130 M^{-1}
3,3′-$Azo_{15}HA$	570 ± 62 M^{-1}	340 M^{-1}

Despite the higher binding affinity of the α-CD HA, we chose to focus on the 4-phenylazobenzoic acid/β-CD binding pairs due to their isomerization properties as described below. Specifically, we designed supramolecular hydrogels to self-assemble from HA modified with 4-phenylazobenzoic acid (Azo_xHA, guest) and β-CD_x-HA (βCD_xHA, host), where "x" denotes the percentage of disaccharides that were modified with either Azo or β-CD. For the work presented here, modification levels of 8%, 20%, and 28% were examined for Azo_xHA, and 28% was used for βCD_xHA, as determined by ^{1}H NMR (Figures S1 and S2). These modification levels were chosen to span a substitution range that still allowed the HA polymer to be fully soluble in aqueous solution and were similar to previous modifications of HA with other guest−host pairs.[32,33]

Because we sought to leverage the Azo isomeric state to control the binding affinity, we next measured K_a for both the irradiated and nonirradiated states of Azo_xHA with β-CD. $Azo_{20}HA$ polymers were titrated by freely soluble β-CD both in the presence and absence of 365 nm irradiation. Complex formation was monitored using ^{1}H NMR spectroscopy, as distinct peaks for the *trans* and *cis* states could be observed (Figures S4 and S5). As demonstrated by the linear fits (Figure 1a), the irradiated *cis* state had an approximately 2.5-fold lower binding affinity for β-CD at 277 M^{-1} compared to 760 M^{-1} for the *trans* state. The decrease in binding affinity indicates that fewer guest−host linkages are thermodynamically favorable when the hydrogel is exposed to 365 nm light, thereby corresponding to a more loosely cross-linked hydrogel. However, the *cis* isomer retains some association with β-CD, allowing the hydrogel to remain intact even with light exposure. Furthermore, it should be noted that complete isomerization to the *cis* state was not achieved, as a significant population of *trans* isomers was present immediately after irradiation (Figure S5). Because the irradiated bulk hydrogel consists of both *cis* and *trans* isomers, the effective binding affinity represents an average of those for both molecular states. Because applications of interest include tuning release profiles or cell culture matrices, we surmised that this change in Azo binding affinity with β-CD was desirable to induce changes in the cross-linking density without the hydrogel undergoing a gel−sol transition.

The absorption spectra of Azo_8HA (Figure 1b) provided further insight into the isomerization behavior of the polymer. In the dark (nonirradiated) state, Azo_8HA showed an absorbance maximum of 325 nm, corresponding to the $\pi-\pi^*$ transition of the *trans* state, and after irradiation with 365 nm light (10 mW/cm^2, 10 min), this peak significantly decreased, and a maximum at 420 nm corresponding to the *cis* n-π transition emerged. Furthermore, upon removal of the light stimulus, there was a slow thermal relaxation process back to

DOI: 10.1021/acs.bioconjchem.7b00802
Bioconjugate Chem. 2018, 29, 905−913

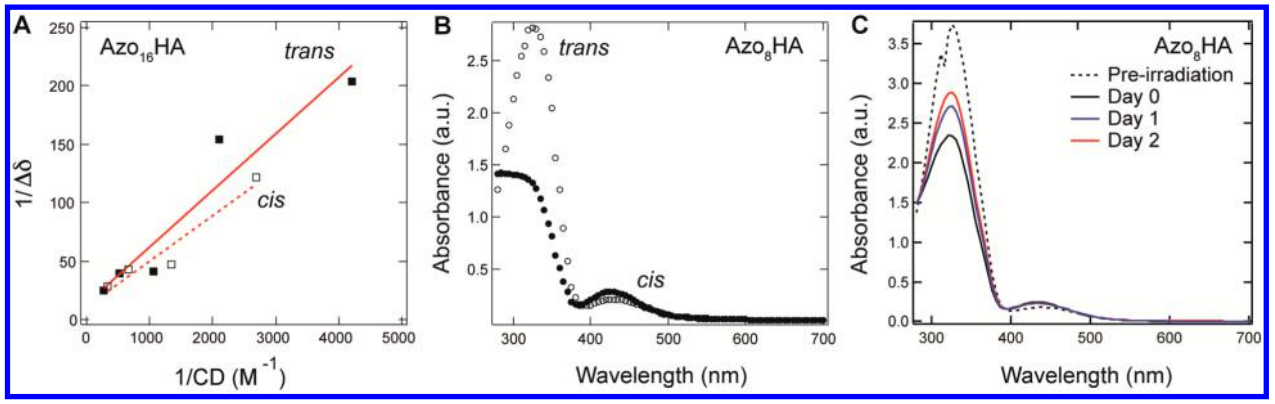

Figure 1. A) The association constant, K_a, determined from linear fits of the NMR shifts of AzoHA protons in the presence of various amounts of free β-CD. As indicated by the linear fits (red lines), the *trans* configuration of the azobenzene demonstrates larger shifts, which corresponds to a higher K_a (760 M^{-1} for *trans* versus 277 M^{-1} for *cis*). B) Absorbance spectra of AzoHA, indicating *trans* Azos with an absorbance maximum at 325 nm and *cis* Azos with decreased absorption at 325 nm and increased absorption at 420 nm. C) After irradiation with 365 nm light for 10 min at 10 mW/cm^2, the Azos in AzoHA relax back to their *trans* configuration.

the *trans* state, which is the more thermodynamically stable isomer (Figure 1c). Consequently, the supramolecular hydrogels do not require constant irradiation and can instead experience short doses of light, thereby minimizing the risk of free radical generation and any subsequent oxidative damage to entrapped biological cargo or cells. For the light doses used here (10 mW/cm^2 and 10 min), previous studies have indicated cytocompatibility and no significant changes to cell phenotype over days to weeks.[34]

Mechanics of Azo-CD Hydrogels. These initial characterization data strongly indicated the potential of supramolecular Azo-βCD_{28}HA hydrogels to exhibit reversible cross-linking and therefore photoswitchable mechanics. Prior to examining photoswitching, we first assessed the mechanics of these hydrogels in the dark state. For all of the hydrogels examined (Figure 2), the guest and host polymers were mixed such that the Azo and CD functional groups were in a 1:1 molar ratio, thereby maximizing the cross-linking density. Similar to other guest–host supramolecular hydrogels,[32] these hydrogels exhibited viscoelastic behavior, as illustrated by the frequency-dependent storage and loss moduli (Figure 2a). Because the guest–host linkage is noncovalent, there is a dynamic equilibrium associated with the binding of Azo in the CD pocket, and the crossover of the storage and loss moduli represents the time scale on which these dynamic bonds rearrange to allow stress dissipation in the bulk material.

For the 7 wt % hydrogels formulated with βCD_{28}HA (Figure 2a), the bulk relaxation time increased as the Azo modification level increased. The fastest relaxation time corresponded to the 8% Azo hydrogel at 0.08 s, while the 20% Azo hydrogel had a relaxation time of 6.2 s. Interestingly, the relaxation time of the Azo_{28}HA hydrogels was long enough to be outside the experimental frequency range, meaning it was on the time scale of at least minutes. As the Azo modification increases in the hydrogel, so does the network connectivity, which will slow polymer mobility and therefore the time scale of relaxation. Of the hydrogels presented here, the Azo_{28}HA hydrogel relaxes stress on a time scale that matches cellular traction force exertion[35] and spreading.[36,37] Furthermore, increasing the modification level of Azo from 8% to 28% resulted in an increase in the overall modulus. This behavior is consistent with a smaller distance between cross-links (higher cross-link density) for the higher modification levels, which corresponds to a more tightly linked network.

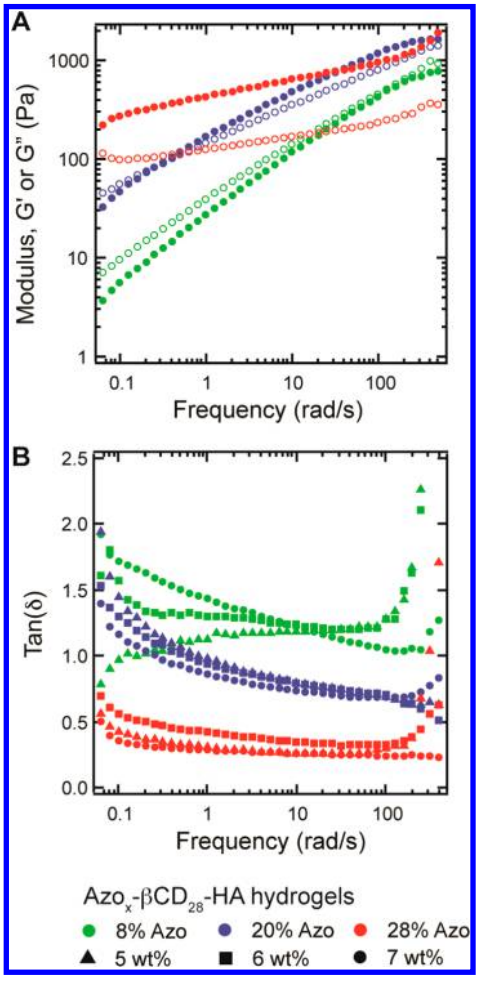

Figure 2. A) Storage (G', closed circles) and loss (G'', open circles) moduli for hydrogels formed with CD_{28}HA and different Azo modifications. Data shown corresponds to 7 wt % hydrogels. B) Ratio of G'' to G' ($\tan(\delta)$) across the experimental frequency range for various Azo modifications and HA concentrations.

Notably, the hydrogels composed of Azo_{28}HA exhibited much more elastic behavior than those composed of either

DOI: 10.1021/acs.bioconjchem.7b00802
Bioconjugate Chem. 2018, 29, 905–913

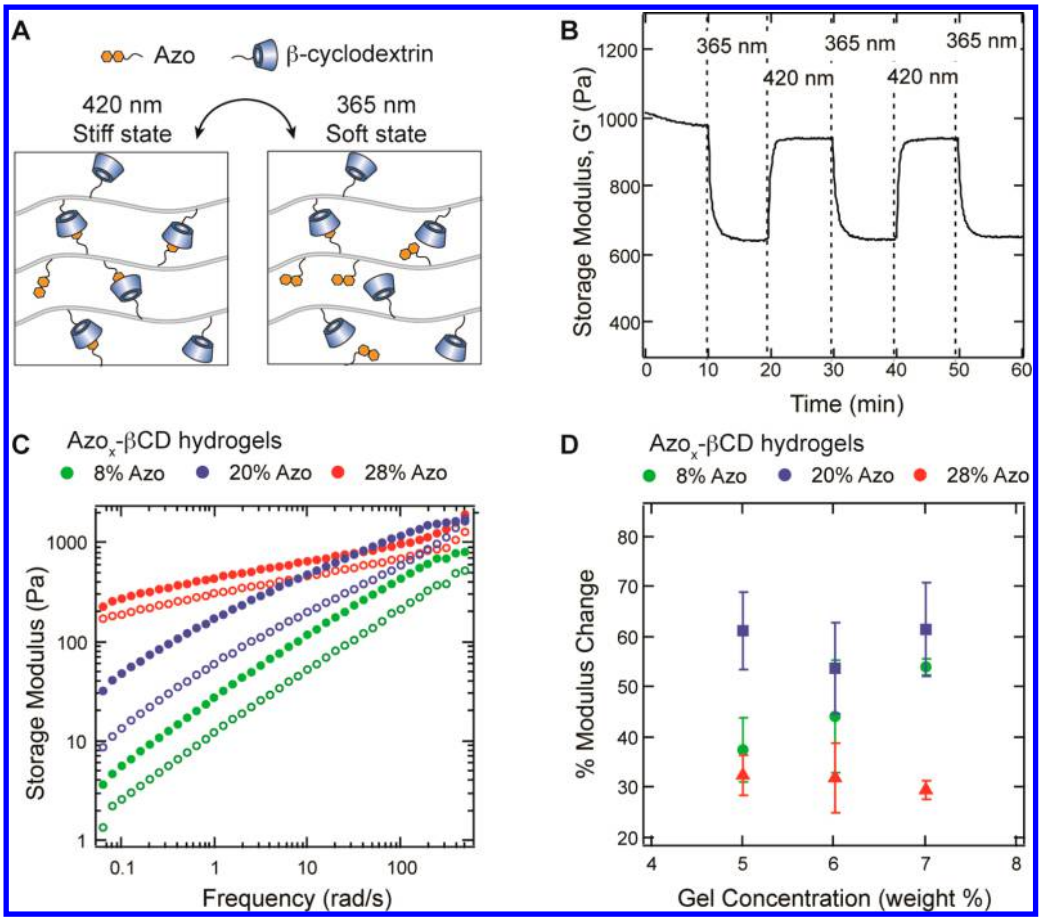

Figure 3. A) Schematic of Azo isomerization within networks upon 365 nm light irradiation, leading to a decreased K_a with CD and a resulting decrease in cross-link density. The isomerization is reversible upon irradiation with visible light (420 nm). B) Example of the reversible change in G' for a 7 wt % Azo$_{28}$-βCD$_{28}$HA hydrogel upon light irradiation with alternating wavelengths (365 nm, 420 nm). G' was measured at 100 rad/s and 1% strain. C) G' before (closed circles) and after (open circles) irradiation across the experimental frequency range for various Azo modifications. D) Magnitude of change in G' upon irradiation for various hydrogel formulations. Data was collected at 10 rad/s and 1% strain.

Azo$_8$HA or Azo$_{20}$HA. For Azo$_{28}$HA, the storage and loss moduli were nearly independent of frequency, and there was a greater disparity between the two (Figure 2a). The ratio of the loss to the storage modulus (defined as tan(δ)) was less than 1 for the Azo$_{28}$HA hydrogels and fairly constant across this frequency range, even for hydrogels containing less polymer overall (down to 5 wt %, Figure 2b). In contrast, tan(δ) for the Azo$_8$HA and Azo$_{20}$HA hydrogels decreased over the experimental frequency range by a factor of 2. Rheology measurements of Azo$_{20}$HA in solution at 7.5 wt % showed a higher storage modulus than loss modulus, indicating that hydrophobic interactions between azobenzene functional groups may contribute to hydrogel mechanical properties at higher modifications (Figure S6). Specifically, previous groups found that $\pi-\pi$ stacking interactions contributed to hydrogel mechanics.[38] These hydrophobic interactions may stabilize the HA polymer chains, thereby decreasing the viscous character of the hydrogel and potentially shifting the dynamic equilibrium of CD complexation.

Photoswitchable Mechanics of Azo-CD Hydrogels. The noncovalent guest−host bonds in these supramolecular hydrogels support a mechanism for the photoswitchability of the number of cross-links. Upon 365 nm irradiation, the Azo units isomerize to the *cis* configuration, shifting the equilibrium of complexation toward removal from the CD cavity (Figure 3a). Dark relaxation or irradiation with visible light (400−500 nm) reverts the azobenzene to its *trans* state and restores the equilibrium that favors complexation.

To probe how these changes in binding affinity affect the storage modulus of the hydrogel, shear oscillatory rheology was performed in the presence of either 365 nm or 400−500 nm irradiation. As an example, the modulus of a 7 wt % hydrogel of Azo$_{28}$-βCD$_{28}$HA was measured at 100 rad/s and 1% strain over time (Figure 3b). Upon irradiation with 365 nm light (10 mW/cm^2), the storage modulus decreased by approximately 36%, indicating the dissociation of Azo units from their CD pockets. Upon switching the light stimulus to 400−500 nm (also 10 mW/cm^2), there was a rapid isomerization back to the *trans* configuration, allowing the hydrogel to recover its initial storage modulus. Multiple cycles (Figure 3b) indicate good reversibility of this process in a range across which previous studies have explored effects on cell phenotype.[39,40] Although this example illustrates the change in storage modulus at one frequency, the percent decrease was the same across all frequencies (Figure 3c, red markers). Interestingly, the loss modulus decreased under 365 nm irradiation as well, although by a smaller percentage (approximately 15%) of the original G''. The decrease in the loss modulus upon irradiation signifies fewer transiently active guest−host interactions, which are known to contribute strongly to the viscous component of the gel mechanics. Overall, however, the greater decrease in G' led to a net increase in tan(δ) across all frequencies (Figure S7), indicating

DOI: 10.1021/acs.bioconjchem.7b00802
Bioconjugate Chem. 2018, 29, 905−913

an increase in the viscous contribution to the hydrogel modulus as expected with the decrease in the number of cross-links.

For lower Azo modifications, G' also decreased in the presence of 365 nm irradiation (Figure 3c). Again, the change in G' before and after irradiation was constant across all frequencies, corresponding to 60% for Azo_{20}-$\beta CD_{28}HA$ hydrogels and 53% for Azo_8-$\beta CD_{28}HA$ hydrogels. When the polymer concentration was varied (Figure 3d), the Azo_{20}-$\beta CD_{28}HA$ and Azo_{28}-$\beta CD_{28}HA$ hydrogels showed constant moduli changes upon irradiation. As noted previously, the relative change in moduli of the Azo_{28}-$\beta CD_{28}HA$ hydrogels was smaller (~36%), perhaps due to the presence of other hydrophobic interactions that do not change upon isomerization. The Azo_8-$\beta CD_{28}HA$ hydrogels, on the other hand, showed an increasing trend in $\Delta G'$ with concentration. For the Azo_8-$\beta CD_{28}HA$ hydrogels, the loss modulus G'' dominated the mechanics in the experimental frequency range at low concentrations, but the 7 wt % hydrogels exhibited a crossover with G' at high frequencies. Because G' is already small at low polymer concentrations, it follows that the change in mechanics caused by UV irradiation is a smaller percentage of the starting modulus.

Model Drug Release and Cytocompatibility. The reversible change in modulus translates to a change in hydrogel cross-linking density and therefore hydrogel mesh size. To investigate the resulting impact on the release properties of these hydrogels, we encapsulated a fluorescently labeled model protein (FITC-BSA) in both Azo_{20}-$\beta CD_{28}HA$ and Azo_{28}-$\beta CD_{28}HA$ hydrogels and measured the cumulative release over time (Figure 4). At day 4, the hydrogels were irradiated with 365 nm light (10 mW/cm^2) for 10 min every hour over 4 h. This pulsed dose of light enabled a sustained change in cross-linking density of the hydrogel over a prolonged time period. As shown in Figure 4a, the Azo_{20}-$\beta CD_{28}HA$ hydrogels showed a burst release of ~45% of total protein released after 1 day. After irradiation at day 4, the irradiated hydrogels released over twice as much protein as the nonirradiated hydrogels (18% vs 7.6%) by day 5. The Azo_{28}-$\beta CD_{28}HA$ hydrogels exhibited similar release behavior (Figure 4b). However, the effect of irradiation on day 4 was not as dramatic, perhaps due to hydrophobic associations within the hydrogel at these higher modifications that do not change with light exposure. For both hydrogel formulations, subsequent release matched that of the nonirradiated hydrogel, likely because many of the cross-links within the irradiated hydrogel reverted back to their *trans* state within a day after the light stimulus was removed. During the experimental time period of a week, none of the hydrogels released 100% of the original amount of FITC-BSA loaded, indicating their potential for sustained delivery. Irradiated hydrogels released more overall due to the decrease in cross-linking density at day 4.

Despite the significant change in modulus upon irradiation (30−60%), the corresponding change in BSA release was relatively modest. One point of note is that the encapsulated protein could be engineered to complex with β-CD, thereby increasing affinity in the hydrogel. Here, however, release is largely dictated by diffusion out of the hydrogel, which itself is degrading by bulk erosion due to the transient nature of the supramolecular cross-links. Interestingly, erosion studies of the hydrogel indicate that HA release is not affected by the irradiation procedure described here (Figure S8). Thus, photomodulation of the azobenzene cross-links has a significant impact on the release due to changes in the mesh size alone. This property sets the stage to improve upon these effects,

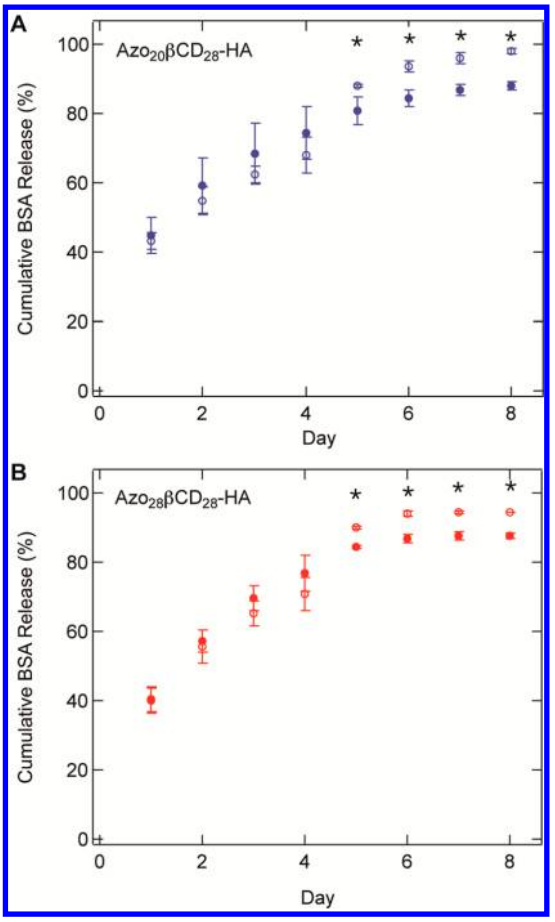

Figure 4. A) Release of FITC-BSA in Azo_{20}-$\beta CD_{28}HA$ hydrogels that were not irradiated (closed circles) or irradiated at day 4 (open circles). Irradiation caused a jump in the amount of FITC-BSA collected at day 5. B) Release of FITC-BSA in Azo_{28}-$\beta CD_{28}HA$ hydrogels that were not irradiated (closed circles) or irradiated at day 4 (open circles). Irradiation also caused a jump in the amount of FITC-BSA collected at day 5, but the effect was diminished compared to Azo_{20}-$\beta CD_{28}HA$ hydrogels.

perhaps by increasing affinity of the model drug for the hydrogel to slow release.

To confirm that this hydrogel platform was suitable for investigations of cellular mechanosensing and more broadly as 3D cell culture matrices, cellular viability was examined using encapsulated NIH 3T3 fibroblasts. The 3T3s were suspended with $Azo_{28}HA$ and then gently mixed with $\beta CD_{28}HA$ to form a 6 wt % cell-laden hydrogel. After culture for 1 day, cell viability was approximately 90% (Figure 5a and 5c). As shown in Figure 5b, this high level of viability was maintained after 3 days of culture; however, the hydrogels experienced some swelling that decreased the overall cell density. These experiments indicate that the designed guest−host hydrogels support 3D encapsulation of live cells.

Cellular morphology remained rounded within the 6 wt % Azo_{28}-$\beta CD_{28}HA$ hydrogels. As previously mentioned, the stress relaxation properties of the hydrogel will affect how the network dissipates cellular traction forces, which in turn affects cell spreading.[35,37] Here, the cellular morphology indicates that the hydrogels are relaxing stress quickly relative to the cells. Increasing the time scale of relaxation with additional cross-links may promote cellular spreading and still maintain reversibility, allowing these hydrogels to be used as platforms

DOI: 10.1021/acs.bioconjchem.7b00802
Bioconjugate Chem. 2018, 29, 905−913

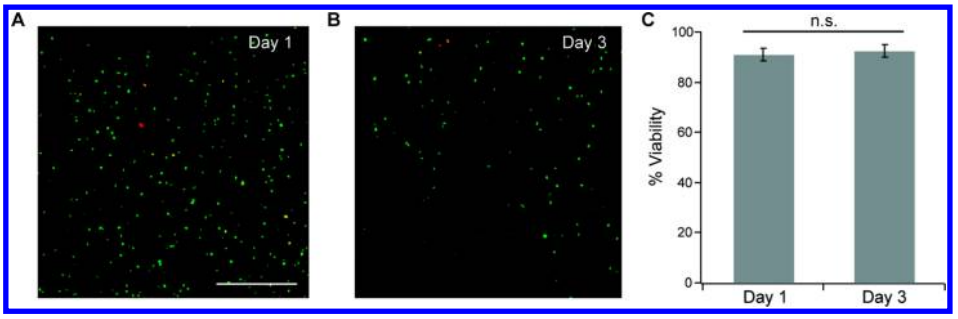

Figure 5. Representative viability of NIH 3T3 fibroblasts encapsulated in a 6 wt % Azo_{28}-βCD_{28}HA hydrogel after A) 1 day and B) 3 days. Fibroblasts are stained with calcein-AM (green, live) or ethidium homodimer (red, dead). The noticeably lower cell density at Day 3 corresponds to hydrogel swelling in media. C) Quantitative viability for NIH 3T3 fibroblasts encapsulated in 6 wt % Azo_{30}-βCD_{28}HA hydrogels after 1 day and 3 days. Error bars represent the standard error of the mean for three hydrogels per condition. Scale bar = 100 μm.

Scheme 1. Synthetic Routes for the Preparation of Azo_xHA (Top) and CD_xHA (Bottom)[a]

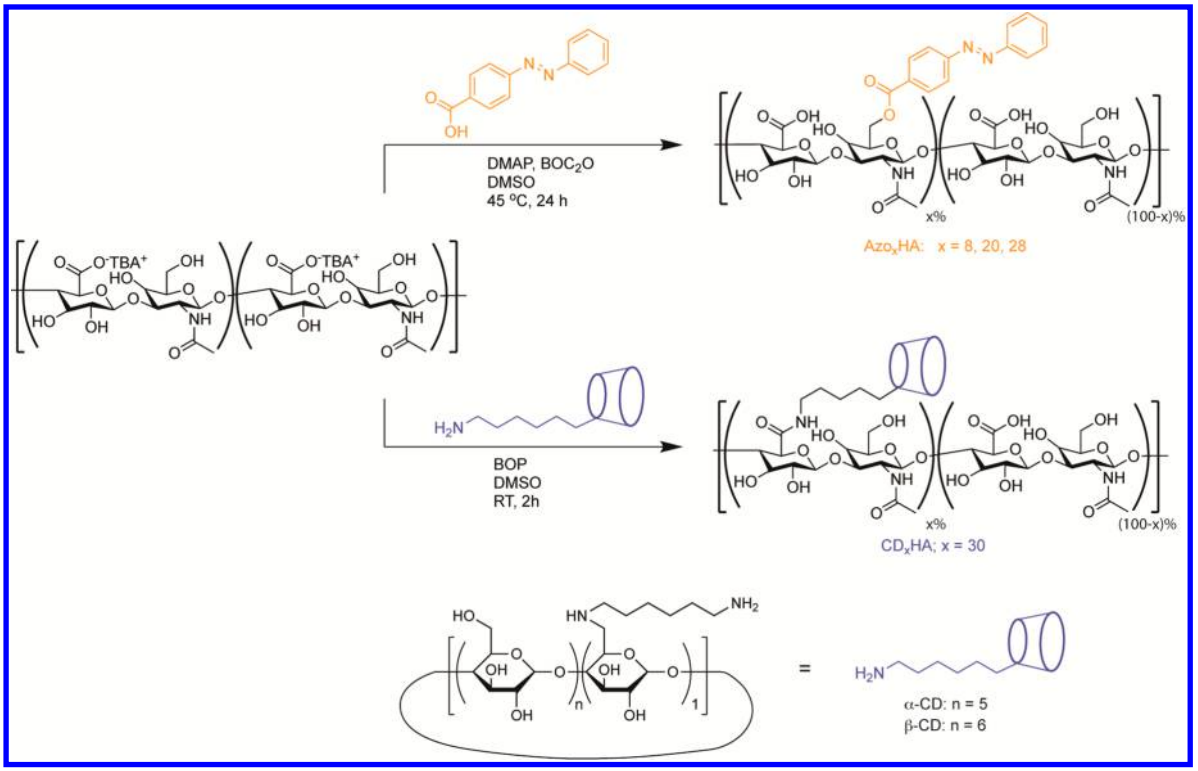

[a]Details for 3,3′-Azo_xHA are found in the SI (Scheme S1). The percentage of HA disaccharides that are modified by the functional group is indicated by "x".

with dynamic mechanical signaling in the future. In addition, the transient nature of the cross-links in the hydrogel could be leveraged to design injectable cell delivery vehicles that flow under shear.[41]

CONCLUSIONS

We designed supramolecular hydrogels using hyaluronic acid polymers functionalized with a photoresponsive guest−host pair: azobenzene and β-cyclodextrin. Increasing modification of HA with Azo substituents decreased the viscoelastic character of the supramolecular hydrogels and led to a lower modulus change upon irradiation. However, all of the hydrogel formulations examined demonstrated reversibility of the cross-linking density, leading to changes in the elastic modulus with light exposure between 36−60%. Importantly, the change in cross-linking density was significant without leading to a gel−sol transition of the material. These reversible changes in cross-linking density were therefore leveraged to tune the release profiles of a model drug, FITC-BSA, with controlled light exposure. In addition, the cytocompatibility of the hydrogel formulations demonstrates the potential of this material strategy to be used for fabrication of dynamic cell culture matrices with temporal control over local matrix mechanics.

MATERIALS AND METHODS

HA Macromer Synthesis. Cyclodextrin-HA (CD_xHA) was synthesized as previously described,[32] and azobenzene-HA (Azo_xHA) was prepared using a similar protocol to others that modify the alcohol groups on HA (Scheme 1). Briefly, for CD_xHA, the *tert*-butylammonium salt of 75 kDa HA (Lifecore) (HA-TBA) was added to a flask with hexanediamine-functionalized α-cyclodextrin or β-cyclodextrin (0.8 eq. to moles of HA-

DOI: 10.1021/acs.bioconjchem.7b00802
Bioconjugate Chem. 2018, 29, 905−913

TBA repeat units) and purged with nitrogen. Anhydrous DMSO (~5 mL per 0.1 g of HA-TBA) was added via cannulation. After the precursors were fully dissolved, (benzotriazol-1-yloxy)tris(dimethylamino)phosphonium hexafluorophosphate (BOP, 0.8 equiv) dissolved in a minimal amount of DMSO was added to the reaction flask. The solution was stirred under nitrogen for 3 h at room temperature, quenched with cold DI water, and transferred to dialysis for purification (~1 week dialysis against water). After 3 days, the polymer solution was centrifuged to remove precipitated byproducts from the coupling. Upon the completion of dialysis, the polymer was freeze-dried and characterized by ^{1}H NMR. Functionalization was determined via integration of the cyclodextrin hexane linker (δ = 1.35−1.85, 12H) relative to the HA methyl singlet (δ = 2.1, 3H), as previously reported (Figure S1).[32]

For Azo$_x$HA, HA-TBA, 4-(phenylazo)benzoic acid or 3,3′-azodibenzoic acid (3 equiv), and 4-dimethylaminopyridine (DMAP, 0.25 equiv) were added to a flask and purged with nitrogen. Anhydrous DMSO (~5 mL per 0.1 g of HA-TBA) was added via cannulation to dissolve the reactants. Upon dissolution, di-*tert*-butyl dicarbonate (Boc_2O, 1.1 equiv, 2.1 equiv, or 3.2 equiv depending on desired functionalization) was added, and the reaction was stirred at 45 °C for 20 h. The reaction was quenched with cold DI water, dialyzed against water for 3 days, and precipitated into cold acetone. The yellow-orange precipitate was redissolved in water and returned to dialysis for an additional 3 days before lyophilization and characterization by ^{1}H NMR. Functionalization was determined via integration of the azobenzene aromatic protons (δ = 7.6−8.4, 9H) relative to the HA methyl singlet (δ = 2.1, 3H) (Figure S2).

Estimation of Binding Affinity with ^{1}H NMR. Azo$_x$HA was dissolved at a concentration of 3.5 mg/mL in DI water and titrated with β-cyclodextrin (0:1, 1:16, 1:8, 1:4, 1:2, and 1:1 ratios of β-cyclodextrin:azobenzene). Samples were lyophilized and redissolved in D_2O. The chemical shift of the azobenzene aromatic protons was then measured using ^{1}H NMR spectroscopy, and the apparent binding affinity (K_a) was estimated using the Benesi−Hildebrand equation

$$\frac{1}{\Delta\delta} = \frac{1}{K_a}\frac{1}{\Delta\delta_{max}[\beta CD]_0} + \frac{1}{\Delta\delta_{max}} \quad (1)$$

where $\Delta\delta$ is the change in chemical shift, and $[\beta CD]_0$ is the total β-cyclodextrin concentration. To determine the binding affinity when the azobenzene was in the *cis* state, samples were irradiated with an Exfo Omnicure S1500 mercury lamp containing a 365 nm light filter (10 mW/cm^2, 10 min) immediately prior to NMR measurement. For each isomeric state (*trans* Azo$_x$HA and *cis* Azo$_x$HA), three independent titrations were performed. Reported values represent the mean ± standard deviation.

Hydrogel Formation. βCD$_x$HA and Azo$_x$HA were separately dissolved in PBS at the desired polymer concentration of the final hydrogel. These components were mixed in a 1:1 ratio of β-cyclodextrin and azobenzene in an Eppendorf tube, using a combination of manual mixing and centrifugation. The gels were allowed to stand for at least 1 day prior to further characterization.

Absorbance Spectroscopy. Absorbance scans of Azo$_x$HA solutions in PBS were run from 280 to 700 nm with a 5 nm step size. To measure the absorbance spectrum after isomerization, solutions were directly irradiated in the plate (365 nm, 10 mW/cm^2, 10 min), and absorbance scans were run immediately after or at defined time points. To determine binding affinity between Azo$_x$HA and soluble α- or β-cyclodextrin, titrations were performed as described above (n = 3 per condition), and the Benesi−Hildebrand method was used by tracking the shift in wavelength of the absorbance maximum.

Rheology. The shear storage and loss moduli of hydrogels ($n \geq 3$ per condition) were measured using an AR2000 rheometer (TA Instruments) with a 20 mm diameter 1° angle cone and plate geometry and a UV light guide accessory. At 1% strain, oscillatory frequency sweeps from 0.01−100 Hz were performed at 25 °C. For measurement of the modulus under irradiation, an Exfo Omnicure S2000 (365 nm, 10 mW/cm^2) was remotely controlled from the rheometer software to expose the sample to light through a quartz plate. Data shown represent typical values for each hydrogel condition.

To illustrate the reversible change in mechanics, the modulus of the hydrogels were monitored over time at 1% strain and 1 rad/s using a Discovery HR-3 rheometer (TA Instruments) with an 8 mm parallel plate geometry. This rheometer was also equipped with a light guide accessory, where the light source was an Exfo Omnicure S1000 with an external filter adapter that contained either a 365 nm filter or a 400−500 nm filter. The filters were manually switched at selected time points, and the intensity of the light was held constant at 10 mW/cm^2.

BSA Release. Release profiles were determined following a procedure similar to previously published methods.[32,41,42] Briefly, fluorescein-labeled bovine serum albumin protein (FITC-BSA) was dissolved in PBS at a concentration of 1 mg/mL, and this solution was used to separately dissolve the Azo$_x$HA and βCD$_x$HA hydrogel precursors. Hydrogels (30 μL each, n = 3 per condition) were then prepared as described above, now encapsulating FITC-BSA. These hydrogels were then loaded into custom fabricated wells made from 3 wt % agarose in a 24 well plate. The wells contained a cylindrical depression that was 5 mm in diameter and 6 mm high that was open to a reservoir of buffer. The hydrogels were covered with 1 mL of PBS and stored at 37 °C. The buffer was removed each day and replaced with fresh PBS. At day 4, one group of the hydrogels was irradiated with 365 nm light (10 mW/cm^2) for 10 min every hour over 4 h (irradiated condition). After the final time point, the gels were dissolved via addition of 5 mg/mL 1-adamantane acetic acid to release any remaining BSA. BSA release was quantified with a plate reader (Infinite M200, Tecan) using 495/525 nm excitation/emission, and fluorescence values were compared to a standard curve to determine total BSA release. Values reported represent the mean ± standard deviation. Significance was determined between the irradiated and nonirradiated conditions using a student's t-test (*$p < 0.05$).

Cell Encapsulation and Microscopy. NIH 3T3 fibroblasts were encapsulated into the hydrogels ($n > 3$) at a density of 5 million cells/mL by mixing the cell suspension with concentrated Azo$_x$HA precursor. The hydrogels were placed into wells formed from 3 wt % agarose, as described above, and the cells were cultured in Media 199 containing 1% fetal bovine serum. Prior to imaging, the cell-laden constructs were incubated with 1 μM calcein-AM (live stain) and 4 μM ethidium homodimer (dead stain) for 20 min. At the desired time points, the cells were imaged using a Leica TCS SP5 confocal microscope. Viability was quantified using the maximum intensity projections from the confocal image z-

DOI: 10.1021/acs.bioconjchem.7b00802
Bioconjugate Chem. 2018, 29, 905−913

stacks and application of Otsu's intensity-based thresholding method with particle (cells) counting via ImageJ.

■ ASSOCIATED CONTENT

Supporting Information

The Supporting Information is available free of charge on the ACS Publications website at DOI: 10.1021/acs.bioconjchem.7b00802.

NMR characterization of the synthesized materials, NMR spectroscopy of AzoHA polymers with cyclodextrin, additional rheology data, HA erosion data (PDF)

■ AUTHOR INFORMATION

Corresponding Author

*E-mail: arosales@che.utexas.edu.

ORCID

Adrianne M. Rosales: 0000-0003-0207-7661

Christopher B. Rodell: 0000-0003-2168-0802

Jason A. Burdick: 0000-0002-2006-332X

Present Addresses

[§]Department of Chemical Engineering, University of Texas at Austin, Austin, TX 78712.

[‖]Center for Systems Biology, Massachusetts General Hospital, Boston, MA 02114.

Notes

The authors declare no competing financial interest.

■ ACKNOWLEDGMENTS

A.M.R. gratefully acknowledges funding from the Burroughs Wellcome Fund PDEP program (award no. 1013981) and a CASI award (award no. 1015895). This work was also supported by the American Heart Association through predoctoral fellowships (C.B.R. and M.H.C.) and the Center for Engineering MechanoBiology through a grant from the National Science Foundation's STC program (CMMI: 15-48571). K.S.A. acknowledges support of this research from a National Science Foundation grant (DMR 1408955).

■ REFERENCES

(1) Burdick, J. A., and Murphy, W. L. (2012) Moving from static to dynamic complexity in hydrogel design. *Nat. Commun. 3*, 1269.

(2) Rosales, A. M., and Anseth, K. S. (2016) The design of reversible hydrogels to capture extracellular matrix dynamics. *Nat. Rev. Mater. 1*, 15012.

(3) Qiu, Z., Yu, H., Li, J., Wang, Y., and Zhang, Y. (2009) Spiropyran-linked dipeptide forms supramolecular hydrogel with dual responses to light and to ligand-receptor interaction. *Chem. Commun. 23*, 3342–3344.

(4) Zhao, F., Bonasera, A., Nöchel, U., Behl, M., and Bléger, D. (2018) Reversible Modulation of Elasticity in Fluoroazobenzene-Containing Hydrogels Using Green and Blue Light. *Macromol. Rapid Commun. 39*, 1700527.

(5) Wu, X., Huang, W., Wu, W.-H., Xue, B., Xiang, D., Li, Y., Qin, M., Sun, F., Wang, W., Zhang, W.-B., et al. (2017) Reversible hydrogels with tunable mechanical properties for optically controlling cell migration. *Nano Res.*, DOI: 10.1007/s12274-017-1890-y.

(6) Zheng, Z., Hu, J., Wang, H., Huang, J., Yu, Y., Zhang, Q., and Cheng, Y. (2017) Dynamic Softening or Stiffening a Supramolecular Hydrogel by Ultraviolet or Near-Infrared Light. *ACS Appl. Mater. Interfaces 9*, 24511–24517.

(7) Rombouts, W. H., de Kort, D. W., Pham, T. T. H., van Mierlo, C. P. M., Werten, M. W. T., de Wolf, F. A., and van der Gucht, J. (2015) Reversible Temperature-Switching of Hydrogel Stiffness of Coassembled, Silk-Collagen-Like Hydrogels. *Biomacromolecules 16*, 2506–2513.

(8) Yoshikawa, H. Y., Rossetti, F. F., Kaufmann, S., Kaindl, T., Madsen, J., Engel, U., Lewis, A. L., Armes, S. P., and Tanaka, M. (2011) Quantitative Evaluation of Mechanosensing of Cells on Dynamically Tunable Hydrogels. *J. Am. Chem. Soc. 133*, 1367–1374.

(9) Abdeen, A. A., Lee, J., Bharadwaj, N. A., Ewoldt, R. H., and Kilian, K. A. (2016) Temporal Modulation of Stem Cell Activity Using Magnetoactive Hydrogels. *Adv. Healthcare Mater. 5*, 2536–2544.

(10) Stowers, R. S., Allen, S. C., and Suggs, L. J. (2015) Dynamic phototuning of 3D hydrogel stiffness. *Proc. Natl. Acad. Sci. U. S. A. 112*, 1953–1958.

(11) Gillette, B. M., Jensen, J. A., Wang, M., Tchao, J., and Sia, S. K. (2010) Dynamic Hydrogels: Switching of 3D Microenvironments Using Two-Component Naturally Derived Extracellular Matrices. *Adv. Mater. 22*, 686–691.

(12) Lin, D. C., Yurke, B., and Langrana, N. A. (2005) Inducing Reversible Stiffness Changes in DNA-crosslinked Gels. *J. Mater. Res. 20*, 1456–1464.

(13) Murphy, W. L., Dillmore, W. S., Modica, J., and Mrksich, M. (2007) Dynamic Hydrogels: Translating a Protein Conformational Change into Macroscopic Motion. *Angew. Chem., Int. Ed. 46*, 3066–3069.

(14) Yuan, W., Yang, J., Kopečková, P., and Kopeček, J. (2008) Smart Hydrogels Containing Adenylate Kinase: Translating Substrate Recognition into Macroscopic Motion. *J. Am. Chem. Soc. 130*, 15760–15761.

(15) Sui, Z., King, W. J., and Murphy, W. L. (2008) Protein-Based Hydrogels with Tunable Dynamic Responses. *Adv. Funct. Mater. 18*, 1824–1831.

(16) Kong, N., Fu, L., Peng, Q., and Li, H. (2017) Metal Chelation Dynamically Regulates the Mechanical Properties of Engineered Protein Hydrogels. *ACS Biomater. Sci. Eng. 3*, 742–749.

(17) Kong, N., Peng, Q., and Li, H. (2014) Rationally Designed Dynamic Protein Hydrogels with Reversibly Tunable Mechanical Properties. *Adv. Funct. Mater. 24*, 7310–7317.

(18) Beharry, A. A., and Woolley, G. A. (2011) Azobenzene photoswitches for biomolecules. *Chem. Soc. Rev. 40*, 4422–4437.

(19) Rosales, A. M., Mabry, K. M., Nehls, E. M., and Anseth, K. S. (2015) Photoresponsive Elastic Properties of Azobenzene-Containing Poly(ethylene-glycol)-Based Hydrogels. *Biomacromolecules 16*, 798–806.

(20) Peng, L., You, M., Yuan, Q., Wu, C., Han, D., Chen, Y., Zhong, Z., Xue, J., and Tan, W. (2012) Macroscopic Volume Change of Dynamic Hydrogels Induced by Reversible DNA Hybridization. *J. Am. Chem. Soc. 134*, 12302–12307.

(21) Kang, H., Liu, H., Zhang, X., Yan, J., Zhu, Z., Peng, L., Yang, H., Kim, Y., and Tan, W. (2011) Photoresponsive DNA-Cross-Linked Hydrogels for Controllable Release and Cancer Therapy. *Langmuir 27*, 399–408.

(22) Rastogi, S. K., Anderson, H. E., Lamas, J., Barret, S., Cantu, T., Zauscher, S., Brittain, W. J., and Betancourt, T. (2017) Enhanced Release of Molecules upon Ultraviolet (UV) Light Irradiation from Photoresponsive Hydrogels Prepared from Bifunctional Azobenzene and Four-Arm Poly(ethylene glycol). *ACS Appl. Mater. Interfaces*, DOI: 10.1021/acsami.6b16183.

(23) Zhao, Y.-L., and Stoddart, J. F. (2009) Azobenzene-Based Light-Responsive Hydrogel System. *Langmuir 25*, 8442–8446.

(24) Yamaguchi, H., Kobayashi, Y., Kobayashi, R., Takashima, Y., Hashidzume, A., and Harada, A. (2012) Photoswitchable gel assembly based on molecular recognition. *Nat. Commun. 3*, 603.

(25) Bortolus, P., and Monti, S. (1987) Photoisomerization of azobenzene-cyclodextrin inclusion complexes. *J. Phys. Chem. 91*, 5046–5050.

(26) Tamesue, S., Takashima, Y., Yamaguchi, H., Shinkai, S., and Harada, A. (2010) Photoswitchable Supramolecular Hydrogels Formed by Cyclodextrins and Azobenzene Polymers. *Angew. Chem., Int. Ed. 49*, 7461–7464.

(27) Guan, Y., Zhao, H.-B., Yu, L.-X., Chen, S.-C., and Wang, Y.-Z. (2014) Multi-stimuli sensitive supramolecular hydrogel formed by host-guest interaction between PNIPAM-Azo and cyclodextrin dimers. *RSC Adv. 4*, 4955−4959.
(28) Bian, Q., Wang, W., Wang, S., and Wang, G. (2016) Light-Triggered Specific Cancer Cell Release from Cyclodextrin/Azobenzene and Aptamer-Modified Substrate. *ACS Appl. Mater. Interfaces 8*, 27360−27367.
(29) Gong, Y.-H., Yang, J., Cao, F.-Y., Zhang, J., Cheng, H., Zhuo, R.-X., and Zhang, X.-Z. (2013) Photoresponsive smart template for reversible cell micropatterning. *J. Mater. Chem. B 1*, 2013−2017.
(30) Voskuhl, J., Sankaran, S., and Jonkheijm, P. (2014) Optical control over bioactive ligands at supramolecular surfaces. *Chem. Commun. 50*, 15144−15147.
(31) Lee, T. T., García, J. R., Paez, J. I., Singh, A., Phelps, E. A., Weis, S., Shafiq, Z., Shekaran, A., del Campo, A., and García, A. J. (2015) Light-triggered in vivo activation of adhesive peptides regulates cell adhesion, inflammation and vascularization of biomaterials. *Nat. Mater. 14*, 352−360.
(32) Rodell, C. B., Kaminski, A. L., and Burdick, J. A. (2013) Rational Design of Network Properties in Guest−Host Assembled and Shear-Thinning Hyaluronic Acid Hydrogels. *Biomacromolecules 14*, 4125−4134.
(33) Park, K. M., Yang, J.-A., Jung, H., Yeom, J., Park, J. S., Park, K.-H., Hoffman, A. S., Hahn, S. K., and Kim, K. (2012) In Situ Supramolecular Assembly and Modular Modification of Hyaluronic Acid Hydrogels for 3D Cellular Engineering. *ACS Nano 6*, 2960−2968.
(34) Bryant, S. J., Nuttelman, C. R., and Anseth, K. S. (2000) Cytocompatibility of UV and visible light photoinitiating systems on cultured NIH/3T3 fibroblasts in vitro. *J. Biomater. Sci., Polym. Ed. 11*, 439−457.
(35) Cameron, A. R., Frith, J. E., and Cooper-White, J. J. (2011) The influence of substrate creep on mesenchymal stem cell behaviour and phenotype. *Biomaterials 32*, 5979−5993.
(36) Mooney, D. J., Langer, R., and Ingber, D. E. (1995) Cytoskeletal filament assembly and the control of cell spreading and function by extracellular matrix. *J. Cell Sci. 108*, 2311−2320.
(37) Chaudhuri, O., Gu, L., Darnell, M., Klumpers, D., Bencherif, S. A., Weaver, J. C., Huebsch, N., and Mooney, D. J. (2015) Substrate stress relaxation regulates cell spreading. *Nat. Commun. 6*, 6365.
(38) Li, F., Zhu, Y., You, B., Zhao, D., Ruan, Q., Zeng, Y., and Ding, C. (2010) Smart Hydrogels Co-switched by Hydrogen Bonds and $\pi-\pi$ Stacking for Continuously Regulated Controlled-Release System. *Adv. Funct. Mater. 20*, 669−676.
(39) Tokuda, E. Y., Leight, J. L., and Anseth, K. S. (2014) Modulation of matrix elasticity with PEG hydrogels to study melanoma drug responsiveness. *Biomaterials 35*, 4310−4318.
(40) Mabry, K. M., Lawrence, R. L., and Anseth, K. S. (2015) Dynamic stiffening of poly(ethylene glycol)-based hydrogels to direct valvular interstitial cell phenotype in a three-dimensional environment. *Biomaterials 49*, 47−56.
(41) Loebel, C., Rodell, C. B., Chen, M. H., and Burdick, J. A. (2017) Shear-thinning and self-healing hydrogels as injectable therapeutics and for 3D-printing. *Nat. Protoc. 12*, 1521.
(42) Mealy, J. E., Rodell, C. B., and Burdick, J. A. (2015) Sustained Small Molecule Delivery from Injectable Hyaluronic Acid Hydrogels through Host-Guest Mediated Retention. *J. Mater. Chem. B 3*, 8010−8019.

DOI: 10.1021/acs.bioconjchem.7b00802
Bioconjugate Chem. 2018, 29, 905−913